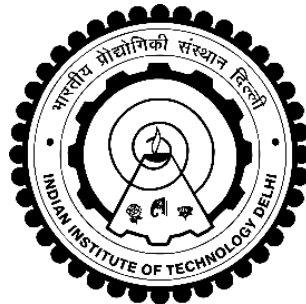


**A HYBRID MULTIOBJECTIVE OPTIMIZATION
APPROACH FOR OPTIMAL DESIGN OF IN- SITU
PERMEABLE REACTIVE BARRIER**

PRATIKSHA PANDEY



**DEPARTMENT OF CIVIL ENGINEERING
INDIAN INSTITUTE OF TECHNOLOGY DELHI**

AUGUST 2017

**HYBRID MULTIOBJECTIVE OPTIMIZATION
APPROACH FOR OPTIMAL DESIGN OF IN- SITU
PERMEABLE REACTIVE BARRIER**

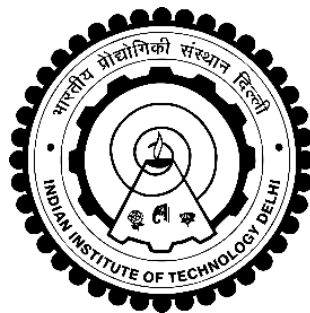
by

PRATIKSHA PANDEY

Department of Civil Engineering

Submitted

**in fulfillment of the requirements of the degree of Doctor of Philosophy
to the**



INDIAN INSTITUTE OF TECHNOLOGY DELHI

AUGUST 2017

Dedicated to

My family

&

Professor Shashi Mathur

(PhD Supervisor)

CERTIFICATE

This is to certify that the thesis, entitled “*Hybrid Multiobjective Optimization Approach for Optimal Design of In- Situ Permeable Reactive Barrier*”, being submitted by **Ms. Pratiksha Pandey** to the Indian Institute of Technology Delhi, for the award of **Doctor of Philosophy**, is a record of bonafide research work carried out by her under my supervision and guidance. The thesis work, in my opinion has reached the standard, fulfilling the requirements for the degree of Doctor of Philosophy. The results contained in this thesis have not been submitted, in part or full, to any other university or institute for the award of any degree or diploma.

(Shashi Mathur)

Professor

Department of Civil Engineering

Indian Institute of Technology Delhi

Hauz Khas, New Delhi – 110016

ACKNOWLEDGMENTS

I deeply express my gratitude to my supervisor Prof. Shashi Mathur for his valuable guidance, constant support and immense patience that inspired me to work smoothly. His deep knowledge in the field of groundwater contamination and fruitful discussions brought many ideas in carrying out my research in the field of Permeable Reactive Barriers. I shall be thankful to him for the rest of my life for helping me in every possible manner to complete this research work at IIT Delhi.

I wish to extend my sincere thanks to the members of my SRC, Prof. K.C. Iyer, Prof. B. R. Chahar and Prof. S.V. Veeravalli for their scientific suggestions which helped me a lot to improve my knowledge. I am very grateful to both Prof. G. V. Ramana and Prof. N. K. Garg for their loving guidance and support in all walks of my life which made my stay at IIT memorable one.

I also want to thank from the bottom of my heart to my dear friend Ms. Anu (Research Scholar, IIT Delhi), for her love, and support during my tough time at IIT Delhi. I would like to extend my thanks to my lab mates Mr. Raktim, Mr. Lohit, Mr. Basant, Mrs. Jyoti, Ms. Vilakshna, Ms. Elisa, Mr. Aniket, Mr. Arvind and Mr. Shushobhit for their love and affection.

I would like to acknowledge my parents for allowing me to grow and fly using my own wings. They supported me constantly and encouraged me a lot to finish this work. I am nothing without you my lovely Mummy and Papa. I would also like to acknowledge my mother-in-law and father-in-law for their sincere support during my stay in the hostel at IIT Delhi.

I sincerely acknowledge the support of my life "Monu" for his unconditional love, patience and faith. I am very thankful to God for blessing me with such a nice and understanding person in my life. He has spent the best and the worst of times with me but his faith in my decisions and my abilities has never wavered. Without you, I would have never been graduated. I am also very thankful for having my brother Ashu. He helped me a lot in the completion of this

work by keeping me enthusiastic and determine towards my research work at every difficult stages.

Pratiksha Pandey

ABSTRACT

A permeable reactive barrier (PRB) is an in situ, innovative and eco-friendly remediation technology that comprises reactive materials to remove contaminants like heavy metals and petroleum hydrocarbons from contaminated groundwater environment. An effective implementation of PRB requires a thorough understanding of the site specific conditions and the associated mass transport processes. Thus, there exists a need to obtain optimal design parameters of PRB under varying distance of the barrier from the source of contamination involving the least possible cost as well as minimum time for remediation (project completion time).

A contaminant transport equation is numerically solved using a finite difference approach with an alternate-direction implicit technique. The developed model is called PRBFD. Later, the developed model is validated and found to perform well. Further, PRBFD is used to simulate a hypothetical case of contamination due to heavy metals. The PRBFD simulations yield the spatial variation (x and y direction) of metal concentration for a duration of 4 years assuming a continuous reactive barrier (CRB) placed near the source. A concentration of 100 mg/l of metal (Zn) is assumed at the source and the distance along the length of the barrier from the source where the Zn concentration reduces to a permissible limit of 5 mg/l is identified. The required length and width of the CRB are subsequently determined after obtaining the plot of the maximum relative concentration in both the x and y directions.

A sensitivity analysis is then conducted to see the impact of various hydraulic parameters (hydraulic conductivity of the barrier, hydraulic gradient, longitudinal and

transverse dispersivity and retardation factor) on the design parameters as well as the total cost of CRB. The maximum length and width of the barrier along with the total cost to clean the metal contaminated site is thus determined.

Later, the PRBFD model is simulated for a BTEX contaminated site with initial BTEX concentration of 100 mg/l and the spatial and temporal variation of the contaminant is plotted up to a maximum period of 6 years. The results obtained are further validated with Visual MODFLOW and a good agreement is observed. Concentration contours are plotted in the absence of a barrier to observe the maximum spread of the plume as it moves towards a monitoring well where a permissible concentration of 1 mg/l is assumed.

Further, a continuous reactive barrier is placed at varying distance from the source and the corresponding length, width and time of remediation required so as to obtain a desired permissible concentration of 1 mg/l at the exit of barrier is determined. A data set is thus generated that provides the length, width and time of remediation for various locations of the barrier as it is moved away from the source.

Following this, a multi-objective optimization algorithm is developed to minimize the two objectives (cost of CRB and the time of remediation) simultaneously. Two different hybrid algorithms developed by combining evolutionary algorithms called HYD-I and HYD-II are proposed in this study. HYD-I is developed by combining Differential Evolution (DE), Particle Swarm Optimization (PSO) and Non-Dominated Sorting Genetic Algorithm (NSGA-II). Similarly, HYD-II is developed by merging Differential Evolution (DE), Particle Swarm Optimization (PSO) and Simulated Annealing (SA) approaches.

The design variables of this study are mainly the length and width of the barrier which are provided to the HYD-I and HYD-II algorithms through an Artificial Neural Network (ANN-I) model so as to achieve fast computations. The ANN-I model is developed by providing approximately 204 sets of inputs (length and width of barrier) and output (time of remediation) that are generated from PRBFD model for a random 204 locations of the barrier from the source.

Similarly, an Artificial Neural Network (ANN-II) model is developed to predict an optimal distance of the barrier from the source for the provided optimal length and width of the barrier as inputs. The two ANN models are used as proxy simulators in the study and thus replace the simulator PRBFD.

Further, combining HYD-I with ANN-I yields a set of paretos of the cost and time of remediation for three different population sizes of 25, 50 and 100. Similarly, HYD-II is linked with ANN-I model to yield a separate set of paretos (cost and time) for a population size of 25, 50 and 100.

The performance of both these hybrid multi-objective optimization algorithms is checked by using four different performance analyzers. The performance analyzers adopted in the study are Inverse Generational Distance (IGD), Spacing, Hyper-volume, and Spread. The performance analyzers yielded a minimum mean value of IGD, Spacing and Spread and a higher mean value of Hyper-volume for HYD-I compared to HYD-II. This indicates that HYD-I performs better than HYD-II or it converges and diverges very well compared to the algorithm HYD-II for a population size of 100.

Later, HYD-I for a population size 100 is further compared with each one of the evolutionary algorithms (NSGA-II, DE and PSO) which initially were combined together to develop HYD-I. Finally, on comparison it is found that the hybrid algorithm HYD-I still performs much better than the individual algorithms.

Subsequently, after establishing the fact that HYD-I performed well for a population size of 100, a set of optimal design variables (length and width of the barrier) are determined for the generated corresponding non-dominated solution (cost and time). Using these design variables, the ANN-II model is used to predict the optimal distance of the barrier from the source. Thus a set of 100 optimal solutions for the length, width, and distance of the barrier from the source along with the cost and time of remediation are generated.

Furthermore, two post pareto approaches are used to determine the best compromising solutions out of the available 100 optimal solutions. A fuzzy logic approach with a maximum linear membership function yields the best optimal cost, time of remediation, optimal length and width of the barrier as well as the optimal distance of the barrier from the source. Similarly, a pseudo weight vector approach is also applied by considering weightage for both the objectives (cost and time). A number of best user specified optimal solutions considering different weightages to the cost and time are suggested for final decision making.

Later, the entire procedure is repeated for different concentrations of BTEX at source to develop design curves. A number of combinations of weights provided to the cost and time are used to prepare design curves to obtain optimal length, width, distance from the source and time of remediation for various finite source

concentrations. Using these design curves, a decision maker could directly pick the values of the optimal parameters for a known source concentration value and subsequently compute the cost incurred.

Finally, a funnel and gate system is also designed so as to compare its cost with the cost obtained for a continuous reactive barrier.

सार

एक पारगम्य प्रतिक्रियात्मक बाधा (पीआरबी) एक स्वस्थानी, अभिनव और पर्यावरण अनुकूल रिमेडियेशन तकनीक है जिसमें प्रदूषित भूजल पर्यावरण से भारी धातुओं और पेट्रोलियम हाइड्रोकार्बन जैसे प्रदूषकों को हटाने के लिए प्रतिक्रियाशील सामग्रियों को शामिल किया गया है। पीआरबी के प्रभावी कार्यान्वयन के लिए साइट विशिष्ट परिस्थितियों और संबंधित जन परिवहन प्रक्रियाओं की संपूर्ण समझ की आवश्यकता है। इस प्रकार, कम से कम संभव लागत के साथ-साथ पुनर्निर्माण के लिए न्यूनतम समय (परियोजना पूरा होने के समय) से संदूषण के स्रोत से बाधा के अलग दूरी के तहत पीआरबी के इष्टतम डिजाइन पैरामीटर प्राप्त करने की आवश्यकता है।

एक संदूषक परिवहन समीकरण संख्यात्मक रूप से एक वैकल्पिक दिशा अंतर्निहित तकनीक के साथ एक सीमित अंतर दृष्टिकोण का उपयोग करके हल किया जाता है। विकसित मॉडल को पीआरबीएफडी कहा जाता है। बाद में, विकसित मॉडल मान्य है और इसे अच्छी तरह से प्रदर्शन करने के लिए पाया जाता है। इसके अलावा, पीआरबीएफडी भारी धातुओं के कारण प्रदूषण का एक काल्पनिक मामला अनुकरण करने के लिए उपयोग किया जाता है। पीआरबीएफडी सिमुलेशन स्रोत के निकट रखा गया एक सतत प्रतिक्रियाशील बाधा (सीआरबी) मानते हुए 4 साल की अवधि के लिए धातु एकाग्रता के स्थानिक भिन्नता (एक्स और वाई दिशा) उपज देते हैं। 100 मिलीग्राम / लीटर धातु (Zn) की एकाग्रता स्रोत और दूरी पर स्रोत से लगाई जाती है, जहां स्रोत की सीमा से Zn एकाग्रता 5 मिलीग्राम / लीटर की अनुमत सीमा तक कम हो जाती है। सीआरबी की आवश्यक लंबाई और चौड़ाई बाद में एक्स और वाई दिशाओं में अधिकतम रिश्तेदार एकाग्रता प्राप्त करने के बाद निर्धारित की जाती है।

डिजाइन मानकों पर सीआरबी की कुल लागत के साथ ही विभिन्न हाइड्रोलिक मापदंडों (Barrier की द्रवचालित प्रवाहिता, द्रवचालित ढाल, अनुदैर्घ्य और अनुक्रमिक विकिरण और मंदता कारक) के प्रभाव को देखने के लिए एक संवेदनशीलता विश्लेषण किया जाता है। धातु की दूषित साइट को साफ करने की कुल लागत के साथ Barrier की अधिकतम लंबाई और चौड़ाई इस प्रकार निर्धारित की जाती है।

बाद में, पीआरबीएफडी मॉडल को BTEX दूषित साइट के लिए 100 मिलीग्राम / लीटर की प्रारंभिक BTEX एकाग्रता के साथ सिम्युलेट किया जाता है और संदूषक के स्थानिक और लौकिक भिन्नता को अधिकतम 6 वर्ष तक प्लॉट किया जाता है। प्राप्त परिणामों को आगे Visual MODFLOW के साथ मान्य किया गया है और एक अच्छा समझौता देखा गया है। plume के अधिकतम फैलाव का पालन करने के लिए एक अवरोध की अनुपस्थिति में एकाग्रता आकृतियां रखी गई हैं क्योंकि यह एक निगरानी की ओर बढ़ती है जहां 1 मिलीग्राम / लीटर की स्वीकार्य एकाग्रता माना जाता है।

इसके अलावा, एक continuous reactive barrier बाधा स्रोत से अलग दूरी और आवश्यक लंबाई, चौड़ाई, और समय की आवश्यकता के लिए आवश्यक है ताकि बाधा के बाहर निकलने पर 1 मिलीग्राम / लीटर की वांछित स्वीकार्य एकाग्रता प्राप्त की जा सके। इस तरह से एक डेटा सेट उत्पन्न होता है जो बाधा के विभिन्न स्थानों के लिए लंबाई, चौड़ाई और समय के उपाय प्रदान करता है क्योंकि यह स्रोत से दूर चलता है।

इसके बाद, एक बहुउद्देशीय अनुकूलन एल्गोरिथ्म को दो उद्देश्यों (सीआरबी की लागत और पुनर्निर्माण के समय) को एक साथ कम करने के लिए विकसित किया गया है। इस अध्ययन में HYD-I और HYD-II नामक विकासवादी एल्गोरिदम के संयोजन के द्वारा दो अलग-अलग संकर एल्गोरिदम का प्रस्ताव रखा गया है। HYD-I को विभेदक विकास (डीई), कण झुंड अनुकूलन (पीएसओ) और गैर-प्रभुत्व छंटनी जेनेटिक एल्गोरिथ्म (एनएसजीए-द्वितीय) के संयोजन के द्वारा विकसित किया गया है। इसी तरह, HYD-II विभेदक विकास (डीई), कण

झुंड अनुकूलन (पीएसओ) और सिमुलेट एनेलिंग (एसए) दृष्टिकोणों को मिलाकर विकसित किया गया है।

इस अध्ययन के डिजाइन चर मुख्य रूप से अवरोध की लंबाई और चौड़ाई हैं जो कि कृत्रिम तंत्रिका नेटवर्क (ANN-I) मॉडल के माध्यम से HYD-I और HYD-II एल्गोरिदम को प्रदान किए जाते हैं ताकि तेजी से कम्प्यूटेशन प्राप्त हो सके। ANN-I मॉडल को लगभग 204 सेटों की आपूर्ति (बाधा की लंबाई और चौड़ाई) और उत्पादन (रीमेडिशन का समय) प्रदान करके विकसित किया गया है जो पीआरबीएफडी मॉडल से स्रोत से अवरोध के 204 स्थानों के यादृच्छिक रूप से उत्पन्न होते हैं।

इसी प्रकार, आर्टिफिशियल न्यूरल नेटवर्क (ANN-II) मॉडल को विकसित किया गया है, जो कि स्रोत से बाधा के इष्टतम दूरी की अनुमानित इष्टतम लंबाई और बाधा की चौड़ाई के लिए अनुमान लगाया गया है। दो एएनएन मॉडलों को अध्ययन में प्रॉक्सी सिमुलेटर के रूप में उपयोग किया जाता है और इस प्रकार सिमुलेटर पीआरबीएफडी को बदल दिया जाता है।

इसके अलावा, ANN-I के साथ HYD-I के संयोजन से 25, 50 और 100 के तीन अलग-अलग आबादी आकारों के लिए लागत और समय के paretos का एक सेट उत्पन्न होता है। इसी प्रकार, HYD-II, ANN-I मॉडल से जुड़ा हुआ है जिससे अलग 25, 50 और 100 के आबादी आकार के लिए paretos (लागत और समय) का सेट उत्पन्न होता है।

इन दोनों संकर बहुउद्देशीय अनुकूलन एल्गोरिदम के प्रदर्शन की जांच चार अलग-अलग प्रदर्शन विश्लेषकों द्वारा की जाती है। अध्ययन में अपनाई जाने वाले निष्पादक विश्लेषणकर्ताओं में उलटा जनरेशनल दूरी (आईजीडी), स्पेसिंग, हाइपर-वॉल्यूम और स्प्रेड शामिल हैं। प्रदर्शन विश्लेषकों ने आईआईजीडी, स्पेसिंग और स्प्रेड का न्यूनतम अर्थ मूल्य और HYD-II के मुकाबले HYD-I के लिए हाइपर-वॉल्यूम के उच्च माध्यम वैल्यू को प्राप्त किया। यह दर्शाता है कि HYD-

I, HYD-II से बेहतर प्रदर्शन करता है या यह 100 के आबादी आकार के लिए एल्गोरिथ्म HYD-II की तुलना में बहुत अच्छी तरह से परिवर्तित हो जाता है।

बाद में, आबादी का आकार 100 के लिए HYD-I को विकासवादी एल्गोरिदम (एनएसजीए-द्वितीय, डीई और पीएसओ) के साथ तुलना में आगे की तुलना की जाती है, जो शुरू में HYD-I को विकसित करने के लिए एक साथ जोड़ दिया गया था। अंत में, तुलना में यह पाया गया है कि हाइब्रिड एल्गोरिथ्म HYD-I अभी भी व्यक्तिगत एल्गोरिदम से बेहतर प्रदर्शन करता है।

इसके बाद, इस तथ्य को स्थापित करने के बाद कि HYD-I, 100 के आबादी आकार के लिए अच्छा प्रदर्शन किया, इष्टतम डिजाइन चर का एक सेट (बाधा का लंबाई और चौड़ाई) तैयार की गई गैर-वर्चस्व वाले समाधान (लागत और समय) के लिए निर्धारित किया गया है। इन डिजाइन चर का उपयोग करके, ANN-II मॉडल को स्रोत से अवरोध के इष्टतम दूरी की भविष्यवाणी करने के लिए उपयोग किया जाता है। इस प्रकार स्रोत से बाधा की लंबाई, चौड़ाई और दूरी के लिए 100 इष्टतम समाधान का एक सेट लागत और रिमैडिशन के समय के साथ उत्पन्न होता है।

इसके अलावा, उपलब्ध 100 इष्टतम समाधानों में से सबसे अच्छा समझौता समाधान निर्धारित करने के लिए दो पोस्ट पारेटो दृष्टिकोण का उपयोग किया जाता है। अधिकतम रेखिक सदस्यता फ़ंक्शन के साथ एक फजी लॉजिक दृष्टिकोण सर्वोत्तम इष्टतम लागत, रिमैडिशन का समय, बाधा के इष्टतम लंबाई और चौड़ाई तथा साथ ही स्रोत से अवरोध का इष्टतम दूरी प्रदान करता है। इसी तरह, एक छद्म वजन वेक्टर दृष्टिकोण दोनों उद्देश्यों (लागत और समय) के लिए भार को ध्यान में रखते हुए भी लागू किया जाता है। अंतिम प्रयोजन के लिए लागत और समय के विभिन्न भारों पर विचार करते हुए इष्टतम समाधान निर्दिष्ट करने वाले सर्वोत्तम उपयोगकर्ता का एक नंबर अंतिम निर्णय लेने के लिए सुझाया गया है।

बाद में, डिजाइन प्रक्रियाओं को विकसित करने के लिए स्रोत पर BTEX के विभिन्न सांद्रणों के लिए पूरी प्रक्रिया दोहराई जाती है। लागत और समय के लिए प्रदान किए गए भार के कई संयोजन, विभिन्न परिमित स्रोत सांद्रता के लिए स्रोत और समय से इष्टतम लंबाई, चौड़ाई, दूरी प्राप्त करने के लिए डिजाइन घटता तैयार करने के लिए उपयोग किए जाते हैं। इन डिजाइनों का इस्तेमाल करना, एक निर्णय निर्माता सीधे ज्ञात स्रोत एकाग्रता मूल्य के लिए इष्टतम पैरामीटर के मूल्यों को चुन सकता है और बाद में खर्च की गणना करता है।

अंत में, एक फ़नल और फाटक सिस्टम भी तैयार किया जाता है ताकि लागत की तुलना में निरंतर प्रतिक्रियाशील बाधा के लिए प्राप्त की जा सके।

TABLE OF CONTENTS

| | |
|--|--------|
| CERTIFICATE | i |
| ACKNOWLEDGMENTS | iii |
| ABSTRACT..... | v |
| TABLE OF CONTENTS..... | xvii |
| LIST OF FIGURES | xxi |
| LIST OF TABLES | xxix |
| NOMENCLATURE | xxxiii |
| ACRONYMS AND ABBREVIATIONS | xxxiv |
| 1 Chapter 1: Introduction | 1 |
| 1.1 General..... | 1 |
| 1.2 Permeable Reactive Barriers | 4 |
| 1.3 Focus of the Study | 8 |
| 1.4 Research Objectives | 9 |
| 1.5 Research Scope..... | 10 |
| 1.6 Organization of the Dissertation..... | 12 |
| 2 Chapter 2: Literature Review | 15 |
| 3 Chapter 3: Model Formulation and Application of Continuous Reactive Barrier for Heavy Metal Removal from Groundwater | 33 |
| 3.1 In-Situ Reactive Barrier for Heavy Metal Removal a General Overview..... | 33 |
| 3.2 Governing Equation..... | 34 |
| 3.3 Solution of Mass Transport Equation using ADI Technique | 34 |
| 3.4 Validation of PRBFD Model..... | 38 |
| 3.5 Assumptions of Numerical Model (PRBFD) | 43 |
| 3.6 Case Study-1: Metal Contamination..... | 44 |
| 3.7 Metal Contaminant Transport without a Barrier | 47 |
| 3.8 Design Curves for a Continuous Reactive Barrier | 51 |
| 3.9 Conclusion..... | 75 |
| 4 Chapter 4: Optimal Design of PRB for BTEX Polluted Groundwater | 77 |
| 4.1 Simulation-Optimization Approach a General Discussion | 77 |

| | | |
|-------|--|-----|
| 4.1.1 | Role of Meta-models in a Simulation–Optimization Process | 78 |
| 4.2 | Study Site..... | 80 |
| 4.3 | Validation of developed model (PRBFD) | 81 |
| 4.4 | Design of the SMZ based Continuous Reactive Barrier..... | 95 |
| 4.5 | Artificial Neural Network (ANN) | 112 |
| 4.5.1 | Learning of Data Set using ANN-I as a Proxy Simulator | 112 |
| 4.5.2 | Learning of Data Set using ANN-II as an Inverse Model..... | 119 |
| 4.6 | Importance of the Multi-objective Optimization..... | 126 |
| 4.6.1 | Multi-objective Model Formulation..... | 126 |
| 4.7 | Hybrid Multi-objective Optimization Algorithm | 129 |
| 4.8 | Proposed Hybrid Optimization Algorithm | 131 |
| 4.9 | Coupled ANN-Hybrid Multi-objective Algorithms | 133 |
| 4.10 | Results obtained using the Proposed Simulation-Optimization Approach | 136 |
| 5 | Chapter 5: Performance Analysis of the Proposed Multi-objective Evolutionary Algorithms..... | 141 |
| 5.1 | Performance Evaluation General Introduction | 141 |
| 5.2 | Performance Analysers..... | 146 |
| 5.3 | Comparison of the Proposed Algorithms using Performance Indicators | 150 |
| 5.4 | Performance Comparison of HYD-I with different evolutionary algorithm..... | 155 |
| 5.5 | Conclusion..... | 160 |
| 6 | Chapter 6: Determination of Best Optimal Solution..... | 161 |
| 6.1 | Overview of Multi-Criteria Decision Making (MCDM)..... | 161 |
| 6.2 | Fuzzy Logic Approach | 162 |
| 6.2.1 | Best Compromising Solution Using Fuzzy Logic Approach..... | 164 |
| 6.3 | Pseudo-Weight Vector Approach..... | 167 |
| 6.4 | Best Compromising Solution Using Pseudo-Weight Vector Approach..... | 170 |
| 6.5 | Conclusion..... | 176 |
| 7 | Chapter 7: Results and Conclusion..... | 177 |
| 7.1 | Optimal CRB Design Curves | 177 |
| 7.2 | Application of Funnel and Gate System..... | 192 |
| 7.3 | Summary and Conclusions | 201 |
| 7.4 | Future Research Recommendations: | 205 |

| | |
|--|-----|
| REFERENCES | 207 |
| (APPENDIX-I) Validation of PRBFD with 2D Numerical Problem | 231 |
| (APPENDIX-II) Spatial and Temporal Variation of Metal Concentration Without Barrier.. | 233 |
| (APPENDIX-III) Spatial and Temporal Variation of Metal Concentration With Barrier..... | 291 |
| (APPENDIX-IV) Temporal Variation of BTEX Concentration in the x and y Directions Obtained from PRBFD and Visual MODFLOW Models..... | 349 |
| (APPENDIX-V) Time of Remediation Obtained from ANN-I and PRBFD Models | 361 |
| (APPENDIX-VI) Distance of Barrier from the Source Obtained from ANN-II and PRBFD Models..... | 363 |
| (APPENDIX-VII) Matlab Code of HYD-I and HYD-II Algorithms | 365 |
| (APPENDIX-VIII) General Description of the Evolutionary Algorithms | 393 |
| (APPENDIX-IX) Paretos Generated by Hybrid Algorithm (HYD-I) for Population Size-100 | 399 |
| (APPENDIX-X) Best Compromising Solution using fuzzy Logic Approach..... | 403 |
| (APPENDIX-XI) Best Compromising Solution using Pseudo Weight Vector Approach | 409 |
| (APPENDIX–XII) Paretos Generated by HYD-I Algorithm for a Case of Source Concentration of 25 mg/l..... | 415 |
| (APPENDIX-XIII) Best Compromising Soution using Pseudo Weight Vector Approach for a case of Source Concentration of 25 mg/l..... | 419 |
| List of Publications | 423 |
| BRIEF BIODATA OF THE AUTHOR..... | 425 |

LIST OF FIGURES

| | |
|--|----|
| Figure 1-1 World water distribution (Gleick, 1996)..... | 1 |
| Figure 1-2 Illustration of permeable reactive barrier..... | 5 |
| Figure 1-3 Design of continuous permeable reactive barrier..... | 6 |
| Figure 1-4 Design of funnel and gate reactive barrier..... | 7 |
| Figure 3-1 Analytical and numerical solution for a one dimensional solute transport..... | 39 |
| Figure 3-2 Comparison of analytically solved concentrations using PRBFD model and Visual MODFLOW at the end of 365 days..... | 41 |
| Figure 3-3 Plan view of site with boundary conditions and well positions (Konikow, 2011)..... | 42 |
| Figure 3-4 Temporal variation of concentration at three locations (A, B and C)..... | 43 |
| Figure 3-5 Schematic diagram of metal contaminated site..... | 44 |
| Figure 3-6 Boundary and initial conditions for a metal source..... | 46 |
| Figure 3-7 Temporal variation of naturally attenuated metal concentration along x direction, with y at 82 m..... | 48 |
| Figure 3-8 Temporal variation of naturally attenuated metal concentration along y direction at various x positions..... | 49 |
| Figure 3-9 Aquifer length along x axis for a permissible relative concentration of 0.05 in the absence of a barrier..... | 50 |
| Figure 3-10 Aquifer width along y axis for a permissible relative concentration of 0.05 in the absence of a barrier..... | 50 |
| Figure 3-11 Barrier length for maximum relative permissible concentration of 0.05..... | 53 |
| Figure 3-12 Barrier width for maximum relative permissible concentration of 0.05..... | 53 |
| Figure 3-13 Barrier length at longitudinal and transverse dispersivities 1 m and 0.1 m..... | 56 |
| Figure 3-14 Barrier width at longitudinal and transverse dispersivities 1 m and 0.1 m..... | 56 |
| Figure 3-15 Barrier length at longitudinal and transverse dispersivities 5 m and 0.5 m..... | 57 |

| | |
|---|----|
| Figure 3-16 Barrier width at longitudinal and transverse dispersivities 5m and 0.5 m..... | 57 |
| Figure 3-17 Barrier length at longitudinal and transverse dispersivities 10 m and 1 m | 58 |
| Figure 3-18 Barrier width at longitudinal and transverse dispersivities 10 m and 1 m..... | 58 |
| Figure 3-19 Barrier length at longitudinal and transverse dispersivities 20 m and 2 m | 59 |
| Figure 3-20 Barrier width at longitudinal and transverse dispersivities 20 m and 2 m..... | 59 |
| Figure 3-21 Maximum metal concentration at 30 Days for different longitudinal and transverse dispersivities of the barrier..... | 60 |
| Figure 3-22 Maximum metal concentration at 180 Days for different longitudinal and transverse dispersivities of the barrier | 60 |
| Figure 3-23 Maximum metal concentration at 1 Year for different longitudinal and transverse dispersivities of the barrier..... | 61 |
| Figure 3-24 Barrier length (24 m) for barrier conductivity 0.01 m/sec | 63 |
| Figure 3-25 Barrier width (16 m) for barrier conductivity 0.01 m/sec | 63 |
| Figure 3-26 Barrier length (20 m) for barrier conductivity 0.0001 m/sec | 64 |
| Figure 3-27 Barrier width (18 m) for barrier conductivity 0.0001 m/sec | 64 |
| Figure 3-28 Barrier length (12 m) for barrier conductivity 0.00001 m/sec | 65 |
| Figure 3-29 Barrier width (20 m) for barrier conductivity 0.00001 m/sec | 65 |
| Figure 3-30 Barrier length (4 m) for barrier conductivity 0.000001 m/sec | 66 |
| Figure 3-31 Barrier length (32 m) for barrier conductivity 0.000001 m/sec | 66 |
| Figure 3-32 Barrier length (26 m) for a hydraulic gradient 0.00833 | 68 |
| Figure 3-33 Barrier width (16 m) for a hydraulic gradient 0.00833 | 69 |
| Figure 3-34 Barrier length (24 m) for a hydraulic gradient 0.005 | 69 |
| Figure 3-35 Barrier length (22 m) for a hydraulic gradient 0.0009 | 70 |
| Figure 3-36 Barrier length (14 m) for a hydraulic gradient 0.0001 | 70 |
| Figure 3-37 Barrier length (10 m) for a hydraulic gradient 0.00009 | 71 |

| | |
|--|----|
| Figure 3-38 Barrier length (58 m) at retardation factor 2 | 72 |
| Figure 3-39 Barrier length (32 m) at retardation factor 5 | 73 |
| Figure 3-40 Barrier length (24 m) at retardation factor 8 | 73 |
| Figure 3-41 Barrier width (16 m) at retardation factor 8 | 74 |
| Figure 3-42 Barrier length (16 m) at retardation factor 15 | 74 |
| Figure 4-1 A view of BTEX contaminated study site..... | 81 |
| Figure 4-2 Schematic plan view of BTEX contaminated site with flow boundaries in the absence of a barrier | 82 |
| Figure 4-3 Finite source (BTEX) with initial and boundary condition of solute..... | 82 |
| Figure 4-4 Initial BTEX concentration parallel to the direction of flow (along x axis) | 84 |
| Figure 4-5 Naturally attenuated BTEX concentration parallel to the direction of flow (along x axis) at y = 108 m after 1 year | 84 |
| Figure 4-6 Naturally attenuated BTEX concentration parallel to the direction of flow (along x axis) at y = 108 m after 3 year | 85 |
| Figure 4-7 Naturally attenuated BTEX concentration parallel to the direction of flow (along x axis) at y = 108 m after 6 years..... | 85 |
| Figure 4-8 Initial BTEX concentration perpendicular to the direction of flow (along y axis) | 86 |
| Figure 4-9 Naturally attenuated BTEX concentration perpendicular to the direction of flow (along y axis) at x = 50 m, after 1 year | 86 |
| Figure 4-10 Naturally attenuated BTEX concentration perpendicular to the direction of flow (along y axis) at x = 112 m, after 3 years | 87 |
| Figure 4-11 Naturally attenuated BTEX concentration perpendicular to the direction of flow (along y axis) at x = 190 m, after 6 years | 87 |
| Figure 4-12 Movement of the BTEX plume towards a monitoring well at various locations and times..... | 94 |

| | |
|--|-----|
| Figure 4-13 Continuous reactive barrier in an aquifer | 96 |
| Figure 4-14 Schematic graph showing barrier distance 140 m from the source | 99 |
| Figure 4-15 Maximum BTEX concentration along the x axis at time 2.5 years with barrier position near to the source | 101 |
| Figure 4-16 Maximum BTEX concentration along the x axis at time 6.7 years with barrier position 140 m away from the source | 102 |
| Figure 4-17 Maximum BTEX concentration along the x axis at time 10 years with barrier position 204 m away from the source | 103 |
| Figure 4-18 Maximum BTEX concentration along the y axis at time 2.5 years with barrier position near to the source | 104 |
| Figure 4-19 Maximum BTEX concentration along the y axis at time 6.7 years with barrier position 140 m away from the source | 105 |
| Figure 4-20 Maximum BTEX concentration along the y axis at time 10 years with barrier position 204 m away from the source | 106 |
| Figure 4-21 Movement of plume after 1 year for the barrier located at a distance of 140 m away from source | 108 |
| Figure 4-22 Movement of plume after 3 years for the barrier located at a distance of 140 m away from source | 109 |
| Figure 4-23 Movement of plume after 4.5 years for the barrier located at a distance of 140 m away from source | 110 |
| Figure 4-24 Movement of plume after 6.7 years for the barrier located at a distance of 140 m away from source | 111 |
| Figure 4-25 General Input-output flow chart of ANN-I with remediation time as a target... | 113 |
| Figure 4-26 Levenberg-Marquardt feedforward backpropagation ANN-I model..... | 113 |
| Figure 4-27 PRBFD simulated remediation time | 114 |

| | |
|--|-----|
| Figure 4-28 Three stages of learning of ANN-I model..... | 116 |
| Figure 4-29 Overall ANN-I performance for remediation time | 117 |
| Figure 4-30 Comparison of simulated PRBFD and predicted ANN-I remediation time | 118 |
| Figure 4-31 Error observed between the predicted ANN-I and simulated PRBFD | 118 |
| Figure 4-32 General input-output flow chart of ANN-II taking distance | 120 |
| Figure 4-33 PRBFD simulated locations of the barrier | 121 |
| Figure 4-34 Three stages of learning of ANN-II model | 123 |
| Figure 4-35 Overall performance of ANN-II for predicting distance of the barrier from the source | 124 |
| Figure 4-36 Comparison of Simulated PRBFD and Predicted ANN-II for distance of barrier from the source | 125 |
| Figure 4-37 Error observed between the predicted ANN-II and simulated PRBFD distance data sets..... | 125 |
| Figure 4-38 Flow diagram of the proposed hybrid optimization algorithm HYD-I | 132 |
| Figure 4-39 Flow diagram of the proposed hybrid optimization algorithm HYD-II..... | 133 |
| Figure 4-40 Coupled simulation-optimization model..... | 134 |
| Figure 4-41 ANN-II model flow chart to determine the optimal distance of the barrier from the source | 135 |
| Figure 4-42 Paretos obtained from the hybrid algorithm HYD-I for different population sizes 25, 50 and 100..... | 138 |
| Figure 4-43 Paretos obtained from the hybrid algorithm HYD-II for different population sizes 25, 50 and 100..... | 139 |
| Figure 5-1 Main criteria of multi-objective optimization problem..... | 142 |
| Figure 5-2 Ideally distributed optimal pareto front..... | 144 |
| Figure 5-3 Poorly distributed but well converged non-dominated solutions..... | 144 |

| | |
|---|-----|
| Figure 5-4 Poorly converged but well diverged non-dominated solutions..... | 145 |
| Figure 5-5 Paretos of curve EF performed better then GH..... | 146 |
| Figure 5-6 Comparison of normalized paretos of HYD-I and HYD-II for population size of 25 | 151 |
| Figure 5-7 Comparison of normalized paretos of HYD-I and HYD-II for population size of 50 | 151 |
| Figure 5-8 Comparison of normalized paretos of HYD-I and HYD-II for population size of 100 | 151 |
| Figure 5-9 Performance comparison using IGD metrics | 158 |
| Figure 5-10 Performance comparison using Spread metrics | 158 |
| Figure 5-11 Performance comparison using Spacing metrics | 159 |
| Figure 5-12 Performance comparison using Hyper-volume metrics..... | 159 |
| Figure 6-1 Working model of Fuzzy Logic | 163 |
| Figure 6-2 A fuzzy logic best compromising solution..... | 166 |
| Figure 6-3 Preferred solution for the cost and time by pseudo weight vector approach | 169 |
| Figure 6-4 Trade-off obtained using HYD-I for a population size 100..... | 171 |
| Figure 6-5 Pseudo weight assigned for their respective non-dominated solutions..... | 173 |
| Figure 7-1 Pareto generated using HYD-I with population size of 100 for..... | 179 |
| Figure 7-2 Pareto generated using HYD-I with population size of 100 for..... | 180 |
| Figure 7-3 Pareto generated using HYD-I with population size of 100 for..... | 180 |
| Figure 7-4 Best optimal CRB length, width and distance from the source for chosen pseudo weightage [cost (100 %) and time (0 %)] at various finite source..... | 183 |
| Figure 7-5 Best optimal CRB length, width and distance from the source for chosen pseudo weightage [cost (85 %) and time (15%)] at various finite source | 183 |

| | |
|--|-----|
| Figure 7-6 Best optimal CRB length, width and distance from the source for chosen pseudo weightage [cost (70 %) and time (30 %)] at various finite source..... | 184 |
| Figure 7-7 Best optimal CRB length, width and distance from the source for chosen pseudo weightage [cost (50 %) and time (50 %)] at various finite source..... | 184 |
| Figure 7-8 Best optimal CRB length, width and distance from the source for chosen pseudo weightage [cost (30 %) and time (70 %)] at various finite source..... | 185 |
| Figure 7-9 Best optimal CRB length, width and distance from the source for chosen pseudo weightage [cost (15 %) and time (85 %)] at various finite source..... | 185 |
| Figure 7-10 Best optimal CRB length, width and distance from the source for a chosen pseudo weightage [cost (0 %) and time (100 %)] at various finite sources | 186 |
| Figure 7-11 Best optimal time of remediation (years) for various chosen pseudo weightages of cost and time at different finite sources | 188 |
| Figure 7-12 Spatial variation of maximum concentration at the end of 8.9 Years in the x direction with a CRB located at a distance of 188 m form the source..... | 190 |
| Figure 7-13 Spatial variation of maximum concentration at the end of 8.9 Years in the y direction | 191 |
| Figure 7-14 Components of a funnel and gate system..... | 192 |
| Figure 7-15 Concentration contours of BTEX after 1 year for a case of FNG placed at a distance of 188 m from the source | 194 |
| Figure 7-16 Concentration contours of BTEX at time 3.5 years for a case of FNG placed at 188 m from the source | 195 |
| Figure 7-17 Concentration contours of BTEX at time 8.9 years for a case of FNG placed at 188 m from the source | 196 |
| Figure 7-18 Spatial variation of maximum concentration at the end of 8.9 Years in the x direction for a funnel and gate located at a distance of 188 m from the source | 197 |

Figure 7-19 Special variation of maximum concentration at the end of 8.9 Years in the y direction with gate width (36 m), width of left and right sections of the funnel (18 m) and total width of the funnel and gate design (72 m) 198

Figure 7-20 Global flow chart linking different components of methodology.....202

LIST OF TABLES

| | |
|--|-----|
| Table 1-1 Estimation of global water distribution (Gleick, 1996) | 2 |
| Table 3-1 Model parameters for a one-dimensional transport problem | 39 |
| Table 3-2 Simulation parameters of a two-dimensional analytical and numerical solute transport problem (Wilson and Miller, 1978) | 40 |
| Table 3-3 Model parameters for a heavy metal study site | 46 |
| Table 3-4 Peak metal concentrations along x axis at the y position of 82 m..... | 48 |
| Table 3-5 Peak metal concentrations along y axis at the various x positions..... | 49 |
| Table 3-6 Unit cost for the cost coefficient used in the multi-objective functions..... | 52 |
| Table 3-7 Impact of longitudinal and transverse dispersivities on the length, width and cost of the barrier | 55 |
| Table 3-8 Impact of hydraulic conductivity of barrier on the length, width and cost of the barrier | 62 |
| Table 3-9 Impact of hydraulic gradient on the length, width and cost of the barrier | 68 |
| Table 3-10 Impact of retardation factor on the length, width and cost of the barrier | 72 |
| Table 4-1 Maximum concentration of BTEX attained due to natural attenuation at various times and locations | 88 |
| Table 4-2 Barrier dimensions and remediation time obtained at different | 100 |
| Table 4-3 Maximum concentration of BTEX in x direction at various times for barrier | 107 |
| Table 4-4 Performance of ANN-I for training, validation and testing of network | 115 |
| Table 4-5 Performance measures to check the overall performance of the ANN-I model.... | 117 |
| Table 4-6 Random data divided by ANN-II for different learning stages for the targeted distance | 121 |
| Table 4-7 Performance of ANN-II for training, validation and testing of network..... | 122 |
| Table 4-8 Performance measures to check the overall performance of the ANN-II model .. | 124 |

| | |
|--|-----|
| Table 4-9 Unit cost for the cost coefficients used in the multi-objective function..... | 127 |
| Table 4-10 Control parameters of different multi-objective algorithms used for designing Hybrid HYD-I and HYD-II algorithms (Oldenhuis, 2010) | 137 |
| Table 5-1 Performance analysers for comparing algorithms HYD-I and HYD-II for the population size 25 | 153 |
| Table 5-2 Performance analysers for comparing algorithms HYD-I and HYD-II for the population size 50 | 154 |
| Table 5-3 Performance analysers for comparing algorithms HYD-I and HYD-II for the population size 100 | 154 |
| Table 5-4 Performance analysers for comparing algorithms HYD-I and other metaheuristic algorithms for the population size 100..... | 156 |
| Table 6-1 Preferred optimal solutions and their pseudo weights..... | 175 |
| Table 6-2 Percentage change in the chosen paretos, optimal design length width and the position of barrier..... | 175 |
| Table 7-1 Best optimal solutions obtained from Pseudo weight vector approach for a finite source of 100 mg/l | 178 |
| Table 7-2 Best optimal solutions obtained from Pseudo weight vector approach for a finite source of 75 mg/l | 181 |
| Table 7-3 Best optimal solutions obtained from Pseudo weight vector approach for a finite source of 50 mg/l | 181 |
| Table 7-4 Best optimal solutions obtained from Pseudo weight vector approach..... | 182 |
| Table 7-5 Best optimal CRB design parameters with optimal distance from the source for calculated Pseudo weightage for Cost (100%) and Time (0%) | 182 |
| Table 7-6 Best optimal remediation time required by CRB chosen based on weightage for the cost and time | 187 |

Table 7-7 Best optimal solutions of CRB design for a finite source concentration of 80 mg/l
.....189

Table 7-8 Cost coefficients of the funnel and gate design.....199

Table 7-9 Design parameters and the cost of both the funnel and gate and200

NOMENCLATURE

| | |
|-----------|--|
| C_{ZVI} | Unit cost for zero valent iron |
| L_B | Length of the barrier |
| W_B | Width of the barrier |
| K_d | Partitioning coefficient |
| C_{CRB} | Cost of the continuous reactive barrier |
| D_x | Longitudinal dispersivity |
| D_y | Transverse dispersivity |
| R_c | Retardation factor |
| λ | Decay rate constant |
| A_T | Thickness of the aquifer |
| C_s | Unit price for the sheet pile segment |
| v | Flow velocity |
| R^2 | Coefficient of determination |
| E | Coefficient of efficiency |
| R | Correlation coefficient |
| C_{SMZ} | Unit cost of the surfactant modified zeolite |
| T_R | Remediation time |
| Zn | Zinc |
| Cu | Copper |
| Pb | Lead |
| Cd | Cadmium |

ACRONYMS AND ABBREVIATIONS

| | |
|---------|--|
| PRB | Permeable Reactive Barrier |
| CRB | Continuous Reactive Barrier |
| FNG | Funnel and Gate System |
| MOIWO | Multi-Objective Invasive Weed Optimization |
| NSGA-II | Non-Dominated Sorting Genetic Algorithm |
| DE | Differential Evaluation |
| PSO | Particle Swarm Optimization |
| SA | Simulated Annealing |
| MCDM | Multi-Criteria Decision Making Technique |
| SMZ | Surfactant Modified Zeolite |
| ZVI | Zero Valent Iron |
| BTEX | Benzene, Toluene, Ethyl Benzene, Xylene |
| HYD-I | Hybrid Multi-Objective Optimization Algorithm-I |
| HYD-II | Hybrid Multi-Objective Optimization Algorithm-II |
| ZVAI | Zero-Valent Aluminum |
| CDDP | Constrained Differential Dynamic Programming |
| NPGA | Niched Pareto Genetic Algorithm |
| GP | Genetic Programming |
| MNN | Modular Neural Network |
| ANN | Artificial Neural Network |
| MOFHS | Multi-Objective Fast Harmony Search |
| EPR | Evolutionary Polynomial Regression |

| | |
|--------|--|
| CMA-ES | Evolutionary Covariance Matrix Adaptation |
| SVM | Support Vector Machine |
| ANFIS | Adaptive Neuro Fuzzy Interface |
| GA | Genetic Algorithm |
| LM | Levenberg-Marquardt |
| RBP | Resilient Back Propagation |
| GD | Generational Distance |
| IGD | Inverted Generational Distance |
| MO | Multi-Objective |
| EA | Evolutionary Algorithms |
| FSBF | Fuzzy Dominance Based Sorting Procedure With A Bacterial Foraging Algorithm |
| SWAT | Soil And Water Assessment Tool |
| ADI | Alternating Direction Implicit Technique |
| PRBFD | A Two Dimensional Numerical Finite Difference Model |
| PCE | Perchloroethylene |
| MSE | Mean Square Error |
| RMSE | Root Mean Square Error |
| MAEP | Mean Absolute Error Percentage |
| RGD | Reversed Generational Distance |